

## An infrared spectroscopic study of the OH stretching frequencies of talc and 10-Å phase to 10 GPa

STEPHEN A. PARRY,<sup>1,\*</sup> ALISON R. PAWLEY,<sup>1,†</sup> RAY L. JONES,<sup>2</sup> AND SIMON M. CLARK<sup>3</sup>

<sup>1</sup>School of Earth, Atmospheric and Environmental Sciences, University of Manchester, Manchester, M13 9PL, U.K.

<sup>2</sup>Daresbury Laboratory, Daresbury, Cheshire WA4 4AD, U.K.

<sup>3</sup>Advanced Light Source, Lawrence Berkeley National Laboratory, Berkeley, California 94720, U.S.A.

### ABSTRACT

The effects of pressure on the OH stretching frequencies of natural talc and two samples of synthetic 10-Å phase have been measured using a diamond-anvil cell and a synchrotron infrared source. The 10-Å phase was synthesized at 6.0–6.5 GPa, 600 °C for 46 hours (sample 10Å-46) and 160 hours (10Å-160). Spectra were collected up to 9.0 GPa (talc), 9.9 GPa (10Å-46), and 9.6 GPa (10Å-160). The OH stretching vibration of Mg<sub>3</sub>OH groups in talc occurs at 3677 cm<sup>-1</sup> at ambient pressure, and increases linearly with pressure at 0.97(2) cm<sup>-1</sup> GPa<sup>-1</sup>. The same vibration occurs in 10-Å phase, but shows negligible pressure shift up to 2 GPa, above which the frequency increases linearly to the maximum pressure studied, at a rate of 0.96(3) cm<sup>-1</sup> GPa<sup>-1</sup> (10Å-46) and 0.87(3) cm<sup>-1</sup> GPa<sup>-1</sup> (10Å-160). Two other prominent bands in the 10-Å phase spectrum are suggested to be due to stretching of interlayer H<sub>2</sub>O, hydrogen-bonded to the nearest tetrahedral sheet. These bands also show little change over the first 2 GPa of compression, as most of the compression of the structure is taken up by closing non-hydrogen bonded gaps between interlayer H<sub>2</sub>O and tetrahedral sheets. Between 2 and 4 GPa, changes in band intensities suggest a rearrangement of the interlayer H<sub>2</sub>O.

**Keywords:** Talc, 10-Å phase, high-pressure studies, IR spectroscopy

### INTRODUCTION

The 10-Å phase is a dense hydrous magnesium silicate with a composition and structure closely related to talc, Mg<sub>3</sub>Si<sub>4</sub>O<sub>10</sub>(OH)<sub>2</sub>, but with the addition of interlayer H<sub>2</sub>O. It was first synthesized by Sclar et al. (1965), at pressures of 3.2–9.5 GPa and temperatures between 375 and 535 °C. Since then, it has been the subject of several studies of its structure and composition, in particular its H<sub>2</sub>O content, and its stability in the system MgO-SiO<sub>2</sub>-H<sub>2</sub>O. The most recent studies (Fumagalli et al. 2001; Comodi et al. 2005) have shown that 10-Å phase has a monoclinic structure comprising talc-like 2:1 tetrahedral:octahedral layers stacked as in phlogopite, i.e., with the tetrahedral rings that form the base of one 2:1 layer lying directly above the tetrahedral rings that form the top of the layer below. H<sub>2</sub>O molecules occupy the interlayer sites. The amount of interlayer H<sub>2</sub>O, indicated by *x* in the formula Mg<sub>3</sub>Si<sub>4</sub>O<sub>10</sub>(OH)<sub>2</sub>·*x*H<sub>2</sub>O, was proposed by Bauer and Sclar (1981) to be *x* = 1, based on thermogravimetric analysis. Later studies suggested that *x* = 2/3 (thermogravimetric analysis: Wunder and Schreyer 1992; Chinnery et al. 1999) or *x* = 2 (weight loss after puncturing capsule: Pawley and Wood 1995). Fumagalli et al. (2001) inferred that the H<sub>2</sub>O content is dependent on synthesis duration. They synthesized 10-Å phase in a set of experiments at 6.7 GPa, 650 °C lasting between 5 minutes and 430 hours. Upon treatment of the run products with acetone, they observed a

swelling behavior that was related to run duration. They inferred that 10-Å phase approaches its maximum H<sub>2</sub>O content by ~300 hours, though they had no means of measuring this H<sub>2</sub>O content. From a single-crystal X-ray refinement of a sample synthesized by Fumagalli et al. (2001) for 360 hours, Comodi et al. (2005) inferred a complete occupancy of the interlayer sites by oxygen, and therefore that *x* = 1.

Comodi et al. (2005) located the O of the interlayer H<sub>2</sub>O at the midpoint between opposing tetrahedral sheets, and suggested that hydrogen bonds point toward two of the basal O atoms of either the upper or lower tetrahedral sheet (model I). However, they noted that the displacement parameter in the refinement of the interlayer O position in the direction perpendicular to the sheets was high, suggesting a positional displacement in this direction. They found that their data were equally well fit with a model in which O positions were displaced by 0.27 Å along *c* (model II). Comodi et al. (2005) also reported that electron microprobe analysis showed a Mg:Si ratio of 3:4, as in talc. A different composition is indicated by a recent synthesis of deuterated 10-Å phase at 6.5 GPa, 600 °C for 400 hours (Pawley et al. 2004; Welch et al. 2006), for which a Mg:Si ratio of 3:3.83(8) was obtained from electron microprobe analysis, indicating a significant Si deficiency relative to talc. At the same time, powder infrared spectroscopy resolved more H environments than expected for the formula Mg<sub>3</sub>Si<sub>4</sub>O<sub>10</sub>(OH)<sub>2</sub>·H<sub>2</sub>O, while <sup>29</sup>Si magic-angle spinning NMR spectroscopy revealed the existence of Si vacancies in the tetrahedral sheets, with around 1 in 20 Si sites vacant. The same <sup>29</sup>Si NMR results were obtained by Kohn and Fumagalli (2002) on one of the samples synthesized

\* Present address: School of Chemistry, University of Manchester, Manchester, M13 9PL, U.K.

† E-mail: alison.pawley@manchester.ac.uk

by Fumagalli et al. (2001).

Recent molecular dynamics modeling of the structure of 10-Å phase (Wang et al. 2004) also indicates a phlogopite-type stacking of the 2:1 layers at ambient conditions. These authors tested models of 10-Å phase with the water contents proposed in previous studies:  $x = 2/3$ , 1, and 2. They showed that structures with both  $x = 1$  and  $x = 2/3$  are stable, but not structures with  $x = 2$ .

High  $P$ - $T$  studies on talc and antigorite have identified 10-Å phase as a breakdown product of these minerals. Pawley and Wood (1995) studied the stability of talc and located the invariant point where talc, 10-Å phase, enstatite, coesite, and water coexist at  $\sim 5$  GPa and 710 °C. Above this pressure 10-Å phase becomes the stable phase with respect to talc. Ulmer and Trommsdorff (1995) observed 10-Å phase in the breakdown products of antigorite from 5.4 to 8 GPa. These studies show that 10-Å phase could be an important storage site for water in subduction zones in the Earth's mantle at pressures beyond the stability of talc and antigorite. Therefore studies of its structural behavior at high pressures are warranted. Here we report the results of an infrared spectroscopic investigation of the compression of 10-Å phase to 10 GPa. We have also investigated the compression of talc. Comparison of its behavior with that of 10-Å phase has aided the interpretation of the 10-Å phase data.

Infrared spectroscopy is the ideal tool to study the behavior of water within a mineral structure, as the stretching vibrations of OH bonds create intense absorption peaks. The development of diamond-anvil cells with diamonds transparent to wavelengths in the OH stretching region provides the means of observing the response of OH stretching frequencies to pressure, and the use of synchrotron radiation sources provides a high beam intensity which allows spectra to be collected from different regions of the sample volume.

Several previous IR studies of talc at ambient pressure have examined the OH stretching region (e.g., Farmer 1974). In pure talc,  $\text{Mg}_3\text{Si}_4\text{O}_{10}(\text{OH})_2$ , there is a single sharp OH stretching frequency of  $\sim 3677$   $\text{cm}^{-1}$ . The high frequency of this vibration is characteristic of a strong OH bond with little or no hydrogen bonding. There is only one band, since all OH groups are in identical environments, with 3 Mg as nearest neighbor cations in a pseudo-trigonal arrangement around the OH. Substitution of other divalent cations for Mg has the effect of lowering the vibrational frequency. Thus for  $\text{Fe}^{2+}$ , additional vibrations at  $\sim 3663$ , 3646, and 3624  $\text{cm}^{-1}$  may occur (Wilkins and Ito 1967), corresponding to OH bonded to 2 Mg + 1 Fe, 1 Mg + 2 Fe, and 3 Fe, respectively. The intensity of the vibration is proportional to the amount of the particular cation configuration.

The first spectroscopic study of 10-Å phase was by Bauer and Sclar (1981), who compared its IR spectrum with that of talc. They observed a sharp peak at 3677  $\text{cm}^{-1}$  in both spectra, but with a lower intensity in the spectrum of 10-Å phase. Additional OH stretching bands were interpreted as being due to hydronium,  $\text{H}_3\text{O}^+$ , its presence attributed to interaction between interlayer  $\text{H}_2\text{O}$  and hydroxyl groups in the 2:1 layer. Much more recently, Fumagalli et al. (2001) collected Raman spectra at ambient conditions of 10-Å phase synthesized for 360 hours. Vibrational frequencies are shown in Table 1. They assigned the 3622  $\text{cm}^{-1}$  band, being the strongest peak, to stretching of OH in

the 2:1 layer. This OH was assumed to be coordinated to 3 Mg in the same way as in talc, with the lower frequency interpreted as being due to the formation of a hydrogen bond to the interlayer water. The other peaks were assigned to vibrations of the interlayer water, with the 3267  $\text{cm}^{-1}$  band assigned to the first overtone of the bending mode, and the other two peaks assigned to OH stretching vibrations. They did not observe any vibrations attributable to hydronium.

The effect of pressure on the OH stretching frequency of talc has been investigated up to 3.5 GPa using Raman spectroscopy by Holtz et al. (1993). They observed a weak positive shift in frequency with pressure, at a rate of 1.1(2)  $\text{cm}^{-1}$   $\text{GPa}^{-1}$ . Comodi et al. (2006) have very recently conducted a Raman spectroscopic study of 10-Å phase to 42 GPa, using material from the same synthesis experiment as used by Fumagalli et al. (2001). The ambient spectrum has the same characteristics as previously published, and the three peaks assigned to OH stretching (3597, 3622, and 3673  $\text{cm}^{-1}$ ) show frequency shifts of  $-0.81$ , 1.91, and 1.38  $\text{cm}^{-1}$   $\text{GPa}^{-1}$ , respectively.

## EXPERIMENTAL METHODS

The samples used in this study were a natural talc and two samples of 10-Å phase. The composition of the talc, determined by electron microprobe analysis, was  $\text{Na}_{0.01}\text{Mg}_{2.93}\text{Fe}_{0.03}\text{Al}_{0.01}\text{Si}_4\text{O}_{10}(\text{OH})_2$ . This is close to ideal, with  $\sim 1\%$  Fe substitution for Mg. The 10-Å phase samples were synthesized from powdered  $\text{Mg}(\text{OH})_2$  and  $\text{SiO}_2$  glass in the ratio 3  $\text{Mg}(\text{OH})_2 + 4 \text{SiO}_2$ , at 6.0–6.5 GPa, 600 °C. One sample (10Å-46) was run for 46 hours, the other (10Å-160) for 160 hours. Both experiments produced fine-grained run products. Powder X-ray diffraction showed complete reaction to 10-Å phase for both samples. The absence of diffraction peaks for other phases (enstatite, coesite) suggests that the Mg:Si ratio is 3:4; however, the samples were too fine-grained to verify this by electron microprobe analysis. The negligible weight loss on puncturing capsules after the synthesis experiments suggested that  $x = 2$  in the 10-Å phase formula, but as this value is much higher than anything that has been previously measured, it must be treated with suspicion. The diffraction peaks from 10Å-160 are sharper than those from 10Å-46, which is consistent with previous studies in which longer run duration produced a more crystalline sample (e.g., Welch et al. 2006). The (001) diffraction peaks are also at slightly higher  $2\theta$  angles, indicating a smaller  $d$ -spacing (e.g., 10.08 and 9.73 Å for  $\text{c}\sin\beta$  in 10Å-46 and 10Å-160, respectively).

Ambient pressure IR spectra were collected for samples pressed into KBr disks and dried at 135 °C (Fig. 1). Backgrounds were corrected by subtraction of the spectrum of a disk of dried KBr only. High-pressure IR spectra were collected using a membrane-type diamond-anvil cell fitted with 300- $\mu\text{m}$  culet, type-1a diamonds, which are transparent to IR wavelengths of 2700–4000  $\text{cm}^{-1}$ . The IR spectra were collected on experimental station 1.4.3 at the Advanced Light Source, U.S.A. The station has a high intensity synchrotron radiation IR source that was collimated to produce a beam  $\sim 10$   $\mu\text{m}$  in diameter. Spectra were collected on a Nicolet Magna

**TABLE 1.** Infrared frequencies in the OH stretching region for 10-Å phase at ambient pressure, together with frequency shifts with pressure and the vibration (all stretching) suggested for each band

$\nu^*$ ( $\text{cm}^{-1}$ )	$\delta\nu/\delta P^\dagger$ ( $\text{cm}^{-1}/\text{GPa}$ )	Suggested stretching vibration	$\nu^\ddagger$ ( $\text{cm}^{-1}$ )
3263	0	Interlayer $\text{H}_2\text{O}$	3267
3591	0	Interlayer $\text{H}_2\text{O}$	3593
3629	1.4(1)	Interlayer $\text{H}_2\text{O}$	3622
3650	?	?	
3668§	$-3.2(5)$	Interlayer $\text{H}_2\text{O}$	3668
3675	$0.87(3)$	Talc-like $\text{Mg}_3\text{OH}$	
3705§	0	?	

Notes: Also shown are equivalent Raman frequencies observed by Fumagalli et al. (2001).

\* This study: 10Å-160.

† All shifts only occur above 2 GPa.

‡ Fumagalli et al. (2001).

§ Only resolved on compression of the sample.

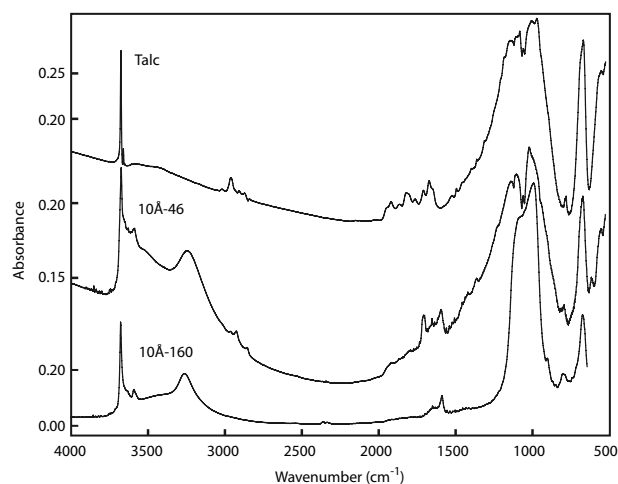


**FIGURE 1.** Background-subtracted ambient-pressure IR spectra of talc and 10-Å phase. Spectra are offset for clarity, with absorbance scales shown for each spectrum. The bands at 2800–3000  $\text{cm}^{-1}$  are from KBr. The bands in the talc spectrum at 1600–2000  $\text{cm}^{-1}$  are assumed to be from  $\text{H}_2\text{O}$  adsorbed onto the sample. The bands in this region in the 10-Å phase spectra are similarly assigned, with the additional band at 1593  $\text{cm}^{-1}$  (10Å-46) and 1591  $\text{cm}^{-1}$  (10Å-160) assigned to interlayer  $\text{H}_2\text{O}$  bending (see text for further discussion).

760 FTIR spectrometer with a resolution of 4  $\text{cm}^{-1}$ . The samples were contained in a 125  $\mu\text{m}$  hole drilled in a stainless steel gasket pre-indented to  $\sim 70$   $\mu\text{m}$  thickness. The samples and KBr pressure medium were dried in an oven at 135  $^\circ\text{C}$  before being loaded into the diamond-anvil cell. After drying, the gasket hole was filled with KBr and the sample was packed into a hole within the KBr. Thus background spectra could be collected at the same pressure conditions as sample spectra. Pressure was determined from the shift of the  $R_1$  ruby fluorescence line (Piermarini et al. 1975) excited by an argon ion laser. To minimize the error in pressure measurement, sample spectra were collected adjacent to a ruby chip used to determine the pressure. Background spectra were collected in areas where there was a low concentration of sample. Pressure was measured before and after collecting each set of IR spectra (sample and background). The run pressure was taken as the average of these two measurements. The pressure error bars shown in Figure 2 are based on a combination of difference in the two pressure measurements, error in measuring the ruby fluorescence peak position, and pressure gradient across the sample. Spectra were collected at pressures up to 9.0, 9.9, and 9.6 GPa for talc, 10Å-46, and 10Å-160, respectively. Spectra were also collected during decompression.

Sample spectra were corrected by subtraction of the KBr spectra collected at the same pressure. Peak positions were then determined by the fitting program Peakfit v4.11 (SYSTAT Software Inc.). The peaks in the talc spectra were fitted using a Voigt function, and the peaks in the 10-Å phase spectra were fitted using an asymmetric double Gaussian fit, which provided the best fit for the strong but asymmetric 3676 and 3591  $\text{cm}^{-1}$  peaks. Each peak was fitted separately by simultaneous fitting of the peak and a progressive linear background. The error in measurement of peak position was  $\pm 0.5$   $\text{cm}^{-1}$ .

## RESULTS

In the OH stretching region, the ambient talc spectrum consists of a strong peak at 3677  $\text{cm}^{-1}$  and a weaker peak at 3660  $\text{cm}^{-1}$  (Fig. 1), which have been assigned to the OH stretching vibration of  $\text{Mg}_3\text{OH}$  and  $\text{Mg}_2\text{FeOH}$  groups, respectively. These assignments are in good agreement with previous studies (e.g., Wilkins and Ito 1967; Petit et al. 2004).

The ambient spectra of the two 10-Å phase samples are similar in the OH stretching region in that they both show a broad peak at  $\sim 3250$ – $3260$   $\text{cm}^{-1}$ , a sharper but weaker peak at 3591  $\text{cm}^{-1}$  and a sharp peak at 3675–3676  $\text{cm}^{-1}$ , i.e., at the same frequency as in talc. The 10Å-160 spectrum also contains very weak peaks

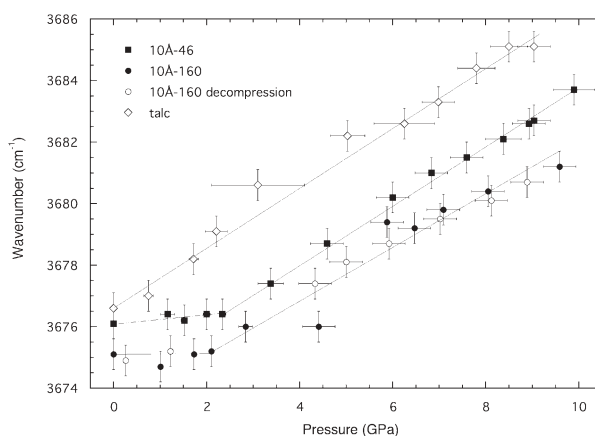


**FIGURE 2.** The stretching frequency of the talc-like OH group in 10-Å phase and talc as a function of pressure. The trends through the data were fit by least-squares, with the 10-Å phase data above 2 GPa fit separately from the data up to 2 GPa. Note that some 10-Å phase points below 2 GPa have not been plotted due to the peak shape being skewed by the presence of a low-frequency shoulder (see text for further discussion).

at 3629 and 3650  $\text{cm}^{-1}$ . A broad hump in both spectra at  $\sim 3400$   $\text{cm}^{-1}$  was assumed to be due to adsorbed atmospheric water, as a much stronger band at the same frequency was present in spectra of undried samples. This band was treated as background. Both spectra also contain a band in the OH bending region that is not present in talc's spectrum (Fig. 1). Below 1500  $\text{cm}^{-1}$  the 10Å-46 and talc spectra are similar to each other, with the 10Å-160 spectrum showing sharper peaks around 1000  $\text{cm}^{-1}$ .

Under pressure in the diamond-anvil cell, the more intense OH stretching vibration in talc moves to higher wavenumber (Fig. 2), at a rate of 0.97(2)  $\text{cm}^{-1}$   $\text{GPa}^{-1}$ . The shift in wavenumber for the weaker OH peak is 0.66(8)  $\text{cm}^{-1}$   $\text{GPa}^{-1}$ . Interference fringes in the spectra of sample 10Å-46 at elevated pressures prevented measurement of the position of all but the sharp 3676  $\text{cm}^{-1}$  peak. Resolution of other peaks was also hampered by dispersal of the 10-Å phase throughout the sample loading. A cleaner sample loading for 10Å-160 allowed resolution of all the OH stretching peaks observed at ambient pressure. Figure 2 shows the frequency shift of the sharp OH stretching peak (hereafter referred to as the main or talc-like band) with pressure for the two 10-Å phase samples. In contrast to talc, this peak does not show a steady increase in frequency. Instead, there is negligible shift up to  $\sim 2$  GPa [0.1(1) and 0.0(2)  $\text{cm}^{-1}$   $\text{GPa}^{-1}$ , for 10Å-46 and 10Å-160, respectively], after which the pressure dependence is approximately the same as for talc [0.96(3) and 0.87(3)  $\text{cm}^{-1}$   $\text{GPa}^{-1}$ ]. The full width at half maximum (FWHM) shows a similar trend. It changes very little from 0–2 GPa, increasing from 6.3  $\text{cm}^{-1}$  at 0 GPa at a rate of 0.2(2)  $\text{cm}^{-1}$   $\text{GPa}^{-1}$ . At higher pressures the peak broadens at a rate of  $\sim 0.5$   $\text{cm}^{-1}$   $\text{GPa}^{-1}$ .

Figure 3 shows a portion of the OH stretching region of the 10Å-160 spectra obtained during compression. This region contains all but one of the observed OH stretching bands. The figure shows that there are major changes to the spectra at 2.1 to 4.4 GPa. Over the pressure interval 0 to 2.1 GPa, all stretching frequencies show no discernible pressure dependence. However, by 2.1 GPa, two other bands are evident, as shoulders on either

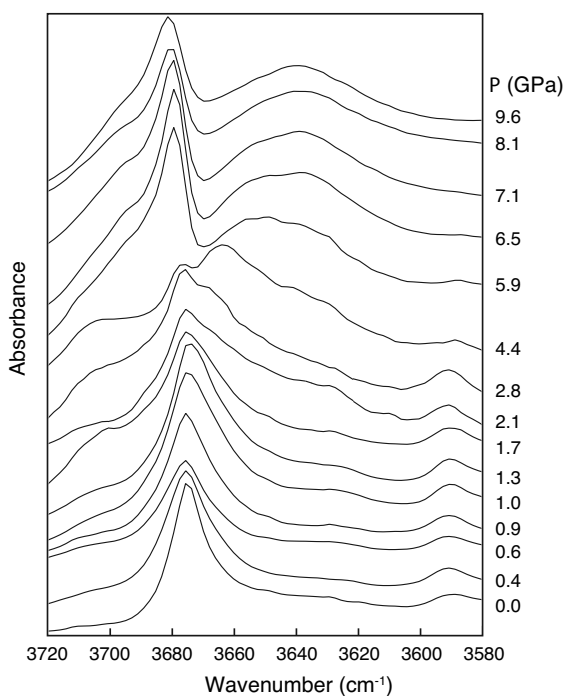


**FIGURE 3.** Evolution of the IR spectra of 10-Å-160 during compression to 9.6 GPa. Spectra are offset for clarity, and the pressure for each spectrum is shown. Intensities have been scaled for clarity, owing to lower absorbance at higher pressure (the intensity of the main talc-like band decreases from  $\sim 0.6$  to  $\sim 0.3$  between 0 and 9.6 GPa, measured from the value at  $3720\text{ cm}^{-1}$  to the peak maximum).

side of the main band, with frequencies of  $\sim 3705$  and  $\sim 3668\text{ cm}^{-1}$ . The  $3705\text{ cm}^{-1}$  band is evident as a very weak shoulder at lower pressures, again showing no obvious pressure dependence. The  $3668\text{ cm}^{-1}$  band is not resolved from the main band below 2.1 GPa, but the broadness of the latter at 1.0 to 1.7 GPa suggests the presence of an overlapping band. This prevented accurate measurement of the position of the main band in some of these spectra, which are therefore omitted from Figure 2.

Above 2.1 GPa the main vibration starts to increase in frequency. However, at 4.4 GPa its frequency is unchanged from that measured in the previous spectrum at 2.8 GPa. From 5.9 to 9.6 GPa it resumes the trend shown by the 2.1 and 2.8 GPa data.

The  $3705$  and  $3591\text{ cm}^{-1}$  bands show no discernible shift in frequency above 2.1 GPa, but their intensities do change. Up to 4.4 GPa the  $3705\text{ cm}^{-1}$  band increases in intensity relative to that of the main band. There then appears to be a discontinuity such that at higher pressures it is no longer evident, though the low resolution means its presence cannot be ruled out. The  $3591\text{ cm}^{-1}$  band decreases in intensity above 2.1 GPa, so that above 6.5 GPa it is no longer resolved.

From 2.1 to 4.4 GPa, the intensities of the  $3668$  and  $3629\text{ cm}^{-1}$  bands increase and then maintain intensity relative to the talc-like band up to the highest pressure investigated. The frequencies of these bands shift continuously to the highest pressure studied, the  $3668\text{ cm}^{-1}$  band to lower frequencies, and the  $3629\text{ cm}^{-1}$  band to higher frequencies. This evolution is not well resolved in Figure 3, owing to overlap of the peaks. However, during

decompression the trend is reversed and the peaks are better resolved. The pressure shifts are shown in Table 1. Extrapolation to high pressures suggests there should be a single peak at  $\sim 9.3$  GPa. In the observed 9.6 GPa spectrum there is indeed a single symmetrical peak.

In all spectra the  $3650\text{ cm}^{-1}$  peak remains very weak and its behavior at high pressure is unclear due to poor resolution and interference fringes in this portion of the spectrum. This peak is therefore not discussed further. Not shown in Figure 3 is the  $3263\text{ cm}^{-1}$  peak from the ambient spectrum. This persists to 1.7 GPa without any noticeable change in frequency. However, it is broad and weak, and at higher pressure it is not possible to resolve above the background interference fringes in the spectra.

During decompression, the main features of the frequency shifts observed during compression are reversed, such that the spectra at 1.2 and 0.2 GPa resemble the low-pressure compression spectra. However, there are insufficient data to determine whether any of the changes previously observed at 2 GPa are reproduced. There is also no sudden change in the frequency of the main OH peak at 4–5 GPa.

## DISCUSSION

### The sharp OH stretching band in talc and 10-Å phase

The main OH stretching band in the talc spectrum at  $3677\text{ cm}^{-1}$  has a uniform positive pressure dependence up to 9.0 GPa, the highest pressure studied. The rate of  $0.97(2)\text{ cm}^{-1}\text{ GPa}^{-1}$  is in agreement with the results of the Raman study of Holtz et al. (1993) up to 3.5 GPa. The positive pressure dependence indicates a shortening and strengthening of the OH bond, suggesting that the hydroxyl groups are not linearly hydrogen-bonded, as otherwise compression would be expected to cause a decrease in O-H $\cdots$ O distances, strengthening of hydrogen bonds, and weakening of the main OH bonds. Pressurization of the sample causes compression of the 2:1 layer, thus reducing the distance between the proton and the Si and/or Mg cations in the surrounding 2:1 layer. The shift in frequency is small because most of the compression of the sample is taken up by the weakly bonded interlayer. The linear frequency increase contrasts with the strong curvature of talc's compressibility in the direction of the OH bonds (Fig. 4a; see also Pawley et al. 1995). The smaller pressure effect for the weaker peak at  $3660\text{ cm}^{-1}$  is inferred to be due either to a lower compressibility of octahedral sites containing  $\text{Fe}^{2+}$  than those containing Mg, resulting in less compression of the associated hydroxyl bonds, or to these OH groups being tilted away from perpendicular orientation relative to the 2:1 layer, and hence experiencing a lower compressibility than the hydroxyl groups associated with 3 Mg.

The relationship between frequency and compressibility for the talc  $\text{Mg}_3\text{OH}$  band is shown in Figure 4b. The curvature of the data shows that interlayer compressibility initially dominates the overall compressibility, but as the interlayer gap closes, compression of the 2:1 layer becomes relatively more important.

The sharp peak in both ambient 10-Å phase spectra is at essentially the same frequency as in talc (Fig. 2). The peak shape is also similar (Fig. 1). These observations suggest that the 10-Å phase peak is equivalent to the talc peak, i.e., it is due to stretching of hydroxyl groups which are coordinated to 3 Mg

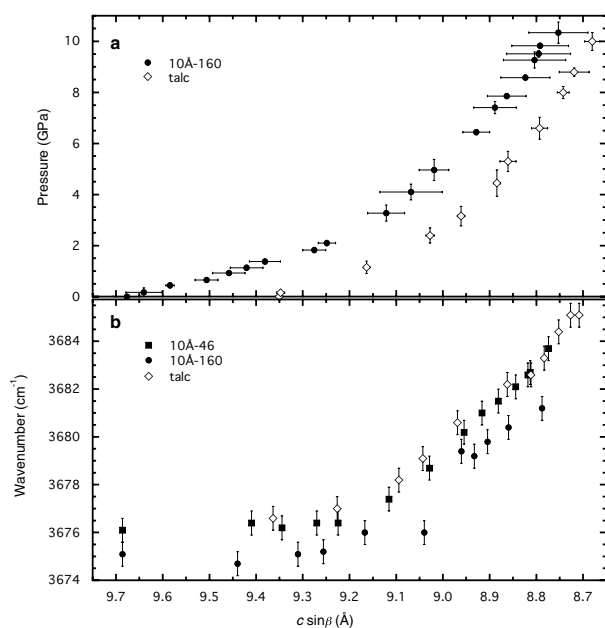


**FIGURE 4.** (a) The basal spacing,  $c \sin \beta$ , of 10-Å phase and talc as a function of pressure (Parry, unpublished). (b) The stretching frequency of the talc-like OH group as a function of  $c \sin \beta$ .  $c \sin \beta$  was obtained by fitting smooth curves to the data in a, and using this relationship to convert the pressures shown in Figure 2 to  $c \sin \beta$ .

in the 2:1 layer of the structure, and which do not interact with interlayer  $\text{H}_2\text{O}$ . An absence of interaction can be explained by the hydroxyl groups facing interlayer  $\text{H}_2\text{O}$  that is too far away to interact. This is the same conclusion as reached by Comodi et al. (2005) for their 10-Å phase model I, in which the distance between the hydroxyl O (O4) and  $\text{H}_2\text{O}$  O (O5) atoms = 3.971 Å, where O5 sits midway between the tetrahedral sheets. Interaction would also be unlikely in the case of their model II, where the O5 site is split along  $c$  into 2 sites separated by 0.54 Å. It could be that some of the hydroxyl groups in 10-Å phase face empty interlayer sites (e.g., if 10-Å phase's  $\text{H}_2\text{O}$  content is  $x = 2/3$ ), but on the basis of the above argument, vibrations of these hydroxyl groups would not be resolvable from hydroxyl groups facing filled sites.

In contrast to our observations and assignment for the talc-like band in 10-Å phase, Fumagalli et al. (2001) and Comodi et al. (2006) observed only a relatively low-intensity peak at similar frequency in their ambient Raman spectra (at 3668 and 3672.5  $\text{cm}^{-1}$  in the two studies, respectively), which they assigned to stretching of interlayer  $\text{H}_2\text{O}$ . In Comodi et al.'s high-pressure study, the intensity increases when moderate pressure is applied, such that their spectrum at 13.1 GPa is similar to ours at 9.6 GPa.

The talc-like OH stretching peak shows a similar shift with pressure as for talc, but only above 2 GPa. Below 2 GPa the behavior is different. Here, the small shift in wavenumber with pressure indicates that there is little shortening of the OH bond length with compression of the structure. This suggests that there is even less compression of the 2:1 layer containing the hydroxyl group than in talc. This is interesting behavior, given that volume data for talc and 10-Å phase show that most of the compression

is perpendicular to the layers in the structure, and that initially 10-Å phase is more compressible in this direction than talc (Fig. 4a). It can therefore be inferred that the greater separation of the 2:1 layers in 10-Å phase than in talc, leads to a greater initial compression in this direction, and that up to 2 GPa essentially all of this compression is taken up by the interlayer.

From 2 GPa to the highest pressures reached (10 GPa for 10-Å phase and 9 GPa for talc), the pressure-dependence of the main OH stretching frequency in 10-Å phase is similar to that observed in talc (excluding the point at 4.4 GPa, discussed in the next section), suggesting similar structure and compressional behavior of the 2:1 layer. The positive pressure-dependence also suggests that the talc-like hydroxyl group in 10-Å phase shows no hydrogen-bonding to the interlayer  $\text{H}_2\text{O}$  up to 10 GPa, since compression of the structure would be expected to lead to strengthening of such a bond. We can examine whether absence of hydrogen bonding is still feasible at 10 GPa by estimating the O4-O5 distance. If we assume that all the compression occurs between O4 and O5, then the data in Figure 4a indicates that from 0 to 10 GPa the interlayer space is compressed by 0.9 Å, and so O4-O5 is compressed by half of this, i.e., 0.45 Å. Using Comodi et al.'s (2005) ambient O4-O5 distance of 3.97 Å (model I), the separation at 10 GPa becomes  $\sim 3.5$  Å. This separation is still too large for any hydrogen bonding to be likely (Libowitzky 1999).

The similarity of the behavior of 10-Å phase above 2 GPa to that of talc is emphasized in Figure 4b, where the 10Å-46 talc-like OH stretching frequency shows the same relationship to  $c \sin \beta$  as the peak in talc itself. The 10Å-160 peak follows the same trend, but at slightly lower frequencies. This figure shows that for both 10-Å phase samples,  $c \sin \beta$  decreases by 0.4–0.5 Å before any compression of the 2:1 layer appears to take place. The subsequent colinearity of the 10Å-46 and talc data suggests that, for a given basal spacing, the occupancy of the interlayer does not affect the structure of the 2:1 layer.

The frequencies of the talc-like band in 10Å-160 are almost all 1–1.5  $\text{cm}^{-1}$  less than for 10Å-46 (Figs. 2 and 4). This could be due to structural differences between the two samples, as evident from the ambient spectra (Fig. 1), which suggest a much closer similarity of the 2:1 layer structure of 10Å-46 to talc than for 10Å-160. Differences are also inferred from the XRD results and from the previous interpretation of increasing  $\text{H}_2\text{O}$  content with run duration (Fumagalli et al. 2001). However, if a structural difference was responsible, we would expect to see contrasting trends with increasing pressure, but we do not. Therefore the difference is considered to be most likely due to the uncertainty on peak fitting.

#### Preliminary assignment of some of the other OH bands in 10-Å phase

Apart from the main talc-like band, the most prominent OH stretching bands in both 10-Å phase spectra at ambient pressure are at  $\sim 3250$ – $3260$  and  $3591$   $\text{cm}^{-1}$  (Fig. 1). We suggest that the former band (at  $3263$   $\text{cm}^{-1}$  in the 10Å-160 spectrum) is assigned to stretching of interlayer  $\text{H}_2\text{O}$ . Fumagalli et al. (2001) assigned their peak at similar frequency to the first overtone of the  $\text{H}_2\text{O}$  bending vibration at  $1593$   $\text{cm}^{-1}$ . We also observe an  $\text{H}_2\text{O}$  bending vibration at this frequency (Fig. 1). However, the greater

intensity and broader shape of the 3263  $\text{cm}^{-1}$  band, together with the observation that the frequency is more than doubled, suggest that the higher frequency band is not an overtone. The clearly resolved OH peak in both of our ambient spectra at 3591  $\text{cm}^{-1}$  also has its equivalent in the spectra of Fumagalli et al. (2001) and Comodi et al. (2006), who assigned it to stretching of interlayer  $\text{H}_2\text{O}$ .

The bands at 3263 and 3591  $\text{cm}^{-1}$  show a similar evolution with pressure. We suggest that they are vibrations of interlayer  $\text{H}_2\text{O}$  in one structural environment. In a mineral in which the  $\text{H}_2\text{O}$  molecules are weakly bonded, symmetric ( $\nu_1$ ) and anti-symmetric ( $\nu_3$ ) stretching modes of  $\text{H}_2\text{O}$  are usually separated by  $\sim 100 \text{ cm}^{-1}$  (e.g., cordierite, Kolesov and Geiger 2000:  $\nu_1 = 3595$  and  $\nu_3 = 3696 \text{ cm}^{-1}$  for class 1, type 1 cordierite). If interaction with the surrounding structure lowers the symmetry, the two OH bonds must be treated separately, and the separation of wavenumber may be up to  $\sim 800 \text{ cm}^{-1}$  (e.g., 2838 and 3612  $\text{cm}^{-1}$  for lawsonite, Libowitzky and Rossman 1996), with the frequency depending on the strength of the hydrogen bonding, such that the lower the frequency, the stronger the hydrogen bond. In this study, hydrogen bond lengths have been estimated from the correlation function of Libowitzky (1999), which suggests that the vibrations at 3263 and 3591  $\text{cm}^{-1}$  correspond to O...O distances of  $\sim 2.73$  and  $>3.0 \text{ \AA}$ , respectively. The former is somewhat shorter than in the models of Comodi et al. (2005). In their model II, in which O positions are displaced along *c* by 0.27  $\text{\AA}$  from the midpoint of the interlayer, hydrogen bonds to the nearer 2:1 layer are 3.01–3.09  $\text{\AA}$  long. If our O...O distances are correct, they imply a significantly asymmetric  $\text{H}_2\text{O}$  position at ambient pressure, with the  $\text{H}_2\text{O}$  molecule possibly displaced perpendicular to [001].

The static frequency of the 3263 and 3591  $\text{cm}^{-1}$  bands over the first 2 GPa of compression of 10 $\text{\AA}$ -160 indicates no change in strength of the bonds over this pressure interval, and hence no change in bond length. This is interpreted as arising from the  $\text{H}_2\text{O}$  molecules being hydrogen bonded to the 2:1 layer on one side only (e.g., Comodi et al.'s model II). As pressure is increased, compression is initially taken up by closing the gap toward the opposing 2:1 layer, without affecting the hydrogen bonds. At around 2 GPa, when 0.4–0.5  $\text{\AA}$  compression along *c* has occurred, the  $\text{H}_2\text{O}$  may be mid-way between the 2:1 layers.

Hydrogen bonding of water molecules to one 2:1 layer is also inferred in the molecular modeling study of Wang et al. (2004) for the two structures stable at ambient conditions ( $x = 2/3$  and 1, both with phlogopite-type stacking), in which the  $\text{H}_2\text{O}$  molecule is slightly closer to the layer to which it is hydrogen bonded.

Above 2 GPa, the bands at 3263 and 3591  $\text{cm}^{-1}$  significantly weaken. At the same time the bands at  $\sim 3668$  and 3629  $\text{cm}^{-1}$  increase in intensity. We suggest that these two peaks are stretching vibrations associated with a different  $\text{H}_2\text{O}$  environment than the one discussed above. Thus, after elimination of the non-hydrogen bonded gap between the interlayer water and tetrahedral sheet at 2 GPa, further pressurization produces a rearrangement in the bonding of the interlayer water to the tetrahedral sheet. The 3668 and 3629  $\text{cm}^{-1}$  bands are in fact present in the ambient spectrum of 10 $\text{\AA}$ -160; however, their intensities are very low, indicating only a small proportion of this  $\text{H}_2\text{O}$  environment. The rapid change in peak intensities at 2–4 GPa suggests that the rearrange-

ment of interlayer  $\text{H}_2\text{O}$  occurs over a short pressure range.

Interestingly, the separation between the 3668 and 3629  $\text{cm}^{-1}$  peaks is only  $\sim 42 \text{ cm}^{-1}$ , indicating similar lengths for the two O-H bonds. This contrasts with the low-pressure arrangement, and suggests a much more symmetrical arrangement of the interlayer  $\text{H}_2\text{O}$  at higher pressure. It is perplexing as to why the peaks proposed as interlayer water stretches at pressures  $>2 \text{ GPa}$  are observed at higher frequency than both of those proposed for the low pressure configuration, as this suggests weaker hydrogen bonding, contrary to the expected high pressure behavior. Perhaps the hydrogen bonding of the interlayer water is perturbed by the approach of the opposing tetrahedral layer, which after elimination of the non-hydrogen bonded gap, should interact more strongly with the interlayer water.

With increasing pressure the new interlayer stretching frequencies follow more predictable changes with pressure, with the 3629  $\text{cm}^{-1}$  peak shifted to higher frequency and the 3668  $\text{cm}^{-1}$  peak shifted to lower frequency. Increased pressure is expected to reduce the separation between the interlayer water and adjacent tetrahedral layer resulting in increased hydrogen bonding between them. If this is the case for only one of the O-H bonds of the interlayer water, it can be expected that the O atom will regain some of its electronegativity and exert a stronger attraction over the other H of the interlayer water, thus shortening this O-H bond length. This trend was observed up to the highest pressure investigated and was reversed on decompression.

The discontinuity in peak intensities at  $\sim 4.4 \text{ GPa}$ , observed in Figure 3, is synchronous with the discontinuity in the frequency of the main talc-like band. There is no concomitant discontinuity in the volume behavior (Fig. 4a), and so it can be inferred that the silicate framework of the structure compresses uniformly through this pressure interval. We cannot explain why the talc-like band shows this discontinuity, as the hydroxyl groups do not interact with the interlayer  $\text{H}_2\text{O}$ . It is also interesting that this behavior is not observed during decompression.

The peak at  $\sim 3705 \text{ cm}^{-1}$ , present as a shoulder on the main OH peak up to 4.4 GPa, represents the most strongly bonded of all the hydroxyl groups in the structure. Its static frequency, where clearly resolved between 1.7 and 4.4 GPa, suggests no interaction with other OH groups. It is interesting that one of the OD stretching vibrations in a sample of deuterated 10- $\text{\AA}$  phase synthesized for 400 hours (Pawley et al. 2004), occurs at 2731  $\text{cm}^{-1}$ , which if it had an equivalent OH vibration, its frequency would be close to 3705  $\text{cm}^{-1}$ , suggesting that this OD ambient-pressure vibration is equivalent to the higher-pressure OH vibration. However, since this band does not occur in the spectrum of talc, it cannot be simply due to vibrations of  $\text{Mg}_3\text{OH}$  with no hydrogen bonding, and it remains enigmatic.

The frequency shifts that we observe up to 9.6 GPa are similar to those observed by Comodi et al. (2006), except they see continuous shifts from ambient pressure, rather than from 2 GPa as we do, and they observe a negative pressure shift for their 3597  $\text{cm}^{-1}$  band (equivalent to the 3593  $\text{cm}^{-1}$  band of Fumagalli et al. 2001, Table 1). While we do not observe any frequency shift for our 3591  $\text{cm}^{-1}$  band, if there were a shift above 2 GPa it would be hard to resolve owing to the rapidly declining intensity. The main difference between our observations and theirs is that, perhaps because we were focusing on a smaller pressure range, we

observed bands at 3705 and 3668  $\text{cm}^{-1}$  that only became resolved at modest pressures. Since the 3705  $\text{cm}^{-1}$  band then disappears at higher pressures while the 3668  $\text{cm}^{-1}$  band merges with the 3629  $\text{cm}^{-1}$  band, our highest pressure spectra are similar to those of Comodi et al. (2006) at 10–13 GPa.

### CONCLUDING REMARKS

Our spectra show that up to  $\sim 2$  GPa there is little change in the environment of any OH group in the 10-Å phase structure. However, in this pressure interval the volume of 10-Å phase compresses by  $\sim 5\%$ , most of this occurring perpendicular to the layers in the structure, such that there is a shortening of  $\sim 0.4$  Å in this direction (Fig. 4). Over this pressure interval we infer that most of the compression is taken up by compaction of the large interlayer spacing. Above 2 GPa, the volume of 10-Å phase follows a similar trend to the volume of talc from ambient pressure. At the same time the stretching frequency of the talc-like hydroxyl group follows a similar trend to the frequency of the band in talc from ambient pressure. Thus talc and 10-Å phase have essentially the same frequency-volume relationships, and the interlayer  $\text{H}_2\text{O}$  has little effect on the 2:1 layers of 10-Å phase, except to push them apart more than in talc. The interlayer  $\text{H}_2\text{O}$  is, however, involved in a rearrangement of its hydrogen bonds to the 2:1 layers at 2–4 GPa, which persists up to 10 GPa, the highest pressure of our spectra.

The stability of 10-Å phase to pressures approximately twice the stability limit of talc is aided not only by its higher density than talc plus water, but also by the hydrogen bonds between the interlayer  $\text{H}_2\text{O}$  and the 2:1 sheets. The rearrangement of the hydrogen bonding at 2–4 GPa presumably helps in the stabilization of 10-Å phase to high pressures.

### ACKNOWLEDGMENTS

This work was supported by NERC studentship NER/S/A/2000/03460 to S.A. Parry, with additional support from CCLRC through a CASE award. We thank M.C. Martin for assistance at beamline 1.4.3 at the ALS. The Advanced Light Source is supported by the Director, Office of Science, Office of Basic Energy Sciences, of the U.S. Department of Energy under contract no. DE-AC02-05CH11231. We thank Annette Kleppe, Sabine Petit, and Associate Editor Eugen Libowitzky for their constructive comments on the manuscript.

### REFERENCES CITED

- Bauer, J.F. and Sclar, C.B. (1981) The "10Å phase" in the system  $\text{MgO-SiO}_2\text{-H}_2\text{O}$ . *American Mineralogist*, 66, 576–585.
- Chinnery, N.J., Pawley, A.R., and Clark, S.M. (1999) In situ observation of the formation of 10 Å phase from talc +  $\text{H}_2\text{O}$  at mantle pressures and temperatures. *Science*, 286, 940–942.
- Comodi, P., Fumagalli, P., Nazzareni, S., and Zanazzi, P.F. (2005) The 10 Å phase: Crystal structure from single-crystal X-ray data. *American Mineralogist*, 90, 1012–1016.
- Comodi, P., Cera, F., Dubrovinsky, L., and Nazzareni, S. (2006) The high-pressure behaviour of the 10 Å phase: A spectroscopic and diffractometric study up to 42 GPa. *Earth and Planetary Science Letters*, 246, 444–457.
- Farmer, V.C. (1974) The layer silicates. In V.C. Farmer, Ed., *The Infrared spectra of minerals*, p. 331–363. Mineralogical Society, London.
- Fumagalli, P., Stixrude, L., Poli, S., and Snyder, D. (2001) The 10Å phase: a high-pressure expandable sheet silicate stable during subduction of hydrated lithosphere. *Earth and Planetary Science Letters*, 186, 125–141.
- Holtz, M., Solin, S.A., and Pinnavaia, T.J. (1993) Effect of pressure on the Raman vibrational modes of layered aluminosilicate compounds. *Physical Review B*, 48, 13312–13317.
- Kohn, S.C. and Fumagalli, P. (2002) New constraints on the structure of 10Å phase from  $^1\text{H}$  and  $^{29}\text{Si}$  MAS NMR data. Abstract WP16, 18<sup>th</sup> IMA meeting, Edinburgh, U.K.
- Kolesov, B.A. and Geiger, C.A. (2000) Cordierite II: The role of  $\text{CO}_2$  and  $\text{H}_2\text{O}$ . *American Mineralogist*, 85, 1265–1274.
- Libowitzky, E. (1999) Correlation of O-H stretching frequencies and O-H...O hydrogen bond lengths in minerals. *Monatshefte Fur Chemie*, 130, 1047–1059.
- Libowitzky, E. and Rossman, G.R. (1996) FTIR spectroscopy of lawsonite between 82 and 325 K. *American Mineralogist*, 81, 1080–1091.
- Pawley, A.R. and Wood, B.J. (1995) The high-pressure stability of talc and 10 Å phase: potential storage sites for  $\text{H}_2\text{O}$  in subduction zones. *American Mineralogist*, 80, 998–1003.
- Pawley, A.R., Redfern, S.A.T., and Wood, B.J. (1995) Thermal expansivities and compressibilities of hydrous phases in the system  $\text{MgO-SiO}_2\text{-H}_2\text{O}$ : Talc, phase A and 10-Å phase. *Contributions to Mineralogy and Petrology*, 122, 301–307.
- Pawley, A.R., Welch, M.D., and Smith, R.I. (2004) The 10-Å phase: Structural constraints from neutron powder diffraction. *Lithos*, 73, S86.
- Petit, S., Martin, F., Wiewiora, A., De Parseval, P., and Decarreau, A. (2004) Crystal-chemistry of talc: A near infrared (NIR) spectroscopy study. *American Mineralogist*, 89, 319–326.
- Piermarini, G.J., Block, S., Barnett, J.D., and Forman, R.A. (1975) Calibration of pressure-dependence of R1 ruby fluorescence line to 195 kbar. *Journal of Applied Physics*, 46, 2774–2780.
- Sclar, C.B., Carrison, L.C., and Schwartz, C.M. (1965) High pressure synthesis and stability of a new hydronium bearing layer silicate in the system  $\text{MgO-SiO}_2\text{-H}_2\text{O}$ . *Eos*, 46, 184.
- Ulmer, P. and Trommsdorff, V. (1995) Serpentine stability to mantle depths and subduction-related magmatism. *Science*, 268, 858–861.
- Wang, J., Kalinichev, A.G., and Kirkpatrick, R.J. (2004) Molecular modeling of the 10-Å phase at subduction zone conditions. *Earth and Planetary Science Letters*, 222, 517–527.
- Welch, M.D., Pawley, A.R., Ashbrook, S.E., Mason, H.E., and Phillips, B.L. (2006) Si vacancies in the 10-Å phase. *American Mineralogist*, 91, 1707–1710.
- Wilkins, R.W.T. and Ito, J. (1967) Infrared spectra of some synthetic talcs. *American Mineralogist*, 52, 1649–1661.
- Wunder, B. and Schreyer, W. (1992) Metastability of the 10-Å Phase in the system  $\text{MgO-SiO}_2\text{-H}_2\text{O}$  (MSH). What about hydrous MSH phases in subduction zones? *Journal of Petrology*, 33, 877–889.

MANUSCRIPT RECEIVED JANUARY 10, 2006

MANUSCRIPT ACCEPTED OCTOBER 23, 2006

MANUSCRIPT HANDLED BY EUGEN LIBOWITZKY